An H_∞ LPV Design for Sampling Varying Controllers : Experimentation with a T Inverted Pendulum

David Robert, Olivier Sename, Daniel Simon

INRIA

INSTITUT NATIONAL DE RECHERCHE EN INFORMATIQUE ET EN AUTOMATIQUE

An H_∞ LPV Design for Sampling Varying Controllers : Experimentation with a T Inverted Pendulum

David Robert — Olivier Sename — Daniel Simon

N° 6380

Décembre 2007

Thème NUM

ISSN 0249-6399 ISRN INRIA/RR--6380--FR+ENG

An H_∞ LPV Design for Sampling Varying Controllers : Experimentation with a T Inverted Pendulum

David Robert *†, Olivier Sename*† , Daniel Simon ‡†

Thème NUM — Systèmes numériques
Équipe-Projet NeCS

Rapport de recherche n° 6380 — Décembre 2007 — 25 pages

Abstract: This report deals with the adaptation of a real-time controller's sampling period to account for the available computing resource variations. The design of such controllers requires a parameter-dependent discrete-time model of the plant, where the parameter is the sampling period. A polytopic approach for LPV (Linear Parameter Varying) systems is then developed to get an H_∞ sampling period dependent controller. A reduction of the polytope size is here performed which drastically reduces the conservatism of the approach and makes easier the controller implementation. Some experimental results on a T inverted pendulum are provided to show the efficiency of the approach.

Key-words: Digital control, linear parameter varying systems, H_∞ control, real experiments.

* GIPSA-lab (Control Systems Dpt.), UMR INPG-CNRS 5216, ENSIEG-BP 46, 38402 Saint Martin d'Hères Cedex, France

† This work is partially supported by the Safe_NeCS project funded by the ANR under grant ANR-05-SSIA-0015-03

‡ INRIA Rhône-Alpes, Inovallée 655 avenue de l'Europe, Montbonnot, 38334 Saint-Ismier Cedex, France

Centre de recherche Inria de Grenoble – Rhône-Alpes
655, avenue de l'Europe, 38334 Montbonnot Saint Ismier (France)
Téléphone : +33 4 76 61 52 00 —Télécopie +33 4 76 61 52 52

Une méthode de conception de contrôleurs à période d'échantillonage variable LPV H_∞ : application à un pendule inversé

Résumé : Ce rapport examine le problème de l'adaptation en temps-réel de la période d'échantillonnage d'un contrôleur, afin de lui permettre de s'adapter aux variations de la ressource de calcul disponible. La conception du contrôleur nécessite d'avoir un modèle en temps discret paramétré du procédé, où le paramètre variable est la période d'échantillonnage. Une méthode basée sur l'approche polytopique (LPV) est utilisée pour synthétiser un contrôleur H_∞ à période variable. L'utilisation d'un polytope de taille réduite permet de réduire fortement le conservatisme et la complexité de reconstruction du contrôleur. La méthode est validée expérimentalement sur un pendule inversé.

Mots-clés : Commande numérique, systèmes à paramètres variables, commande H_∞, validation expérimentale

1 Introduction

High-technology applications (cars, household appliances..) are using more and more computing and network resources, leading to a need of consumption optimisation for decreasing the cost or enhancing reliability and performances. A solution is to improve the flexibility of the system by on-line adaptation of the processor/network utilisation, either by changing the algorithm or by adapting the sampling period. This paper deals with the latter case and presents the synthesis of a control law with varying sampling period.

Few recent works have been devoted to the computing resource variations. In [1] a feedback controller with a sampling period dependent PID controller is used. In [2, 3] a feedback scheduler based on a LQ optimisation of the control tasks periods is proposed. In [4] a processor load regulation is proposed and applied for real-time control of a robot arm. The design of a sampling period dependent RST controller was proposed in [5]. This latter paper dealt with the control of linear SISO systems at a variable sampling rate, and its promising results called for extensions towards multivariable systems.

The presented contribution enhances a previous paper ([6]) using a linear parameter-varying (LPV) approach of the linear robust control framework [7]. The LPV approach primarily deals with variations of the plant's parameters, although it has been applied also to a plant parameter dependent sampling via a lifting technique as in [8].

This paper provides a methodology for designing a sampling period dependent controller with performance adaptation, which can be used in the context of embedded control systems. First we propose a parametrised discretization of the continuous time plant and of the weighting functions, leading to a discrete-time sampling period dependent augmented plant. In particular the plant discretization approximates the matrix exponential by a Taylor series of order N. Therefore we obtain a polytopic LPV model made of 2^N vertices, as presented in [6]. In this paper we exploit the dependency between the variables parameters, which are the successive powers of the sampling period $h, h^2, ..., h^N$, to reduce the number of controllers to be combined to $N+1$. The H_∞ control design method for polytopic models [7] is then used to get a sampling period dependent discrete-time controller. The reduction of the polytopic set drastically decreases both the complexity and the conservatism of the previous work and makes the solution easier to implement. This approach is then validated by experiments on real-time control of a T inverted pendulum.

The outline of this paper is as follows. Section 2 describes the plant discretization and the reduction of the original complexity using the parameters dependency. In section 3 the closed-loop objectives are stated and expressed as weighting functions in the H_∞ framework. Section 4 comments briefly the augmented plant and gives background on H_∞/LPV control design. The experiments on the "T" inverted pendulum are described in section 5. Finally, the paper ends with some conclusions and further research directions.

2 A sample dependent LPV discrete-time model

In this section the way to obtain a polytopic discrete-time model, the parameter of which being the sampling period, is detailed.

We consider a state space representation of continuous time plants as :

$$G : \left\{ \begin{array}{rcl} \dot{x} & = & Ax + Bu \\ y & = & Cx + Du \end{array} \right. \tag{1}$$

where $x \in \mathbb{R}^n$, $u \in \mathbb{R}^m$ and $y \in \mathbb{R}^p$. The exact discretization of this system with a zero order hold at the sampling period h leads to the discrete-time LPV system (2)

$$G_d : \left\{ \begin{array}{rcl} x_{k+1} & = & A_d(h)\, x_k + B_d(h)\, u_k \\ y_k & = & C_d(h)\, x_k + D_d(h)\, u_k \end{array} \right. \tag{2}$$

with

$$\begin{array}{ll} A_d = e^{Ah} & B_d = \displaystyle\int_0^h e^{A\tau} d\tau B \\ C_d = C & D_d = D \end{array} \tag{3}$$

The state space matrices are usually computed using expression (4) and (5), see [9].

$$\begin{pmatrix} A_d & B_d \\ 0 & I \end{pmatrix} = exp\left(\begin{pmatrix} A & B \\ 0 & 0 \end{pmatrix} h \right) \tag{4}$$

$$C_d = C \qquad D_d = D \tag{5}$$

with h ranging in $[h_{min}; h_{max}]$[1]. However in (4) A_d and B_d are not affine on h.

2.1 Preliminary approach: Taylor expansion

Our aim is to get a polytopic model in order to satisfy one of the frameworks of H_∞ control for LPV systems. We here propose to approximate the matrix exponential by a Taylor series of order N as :

$$A_d(h) \approx I + \sum_{i=1}^{N} \frac{A^i}{i!}\, h^i \tag{6}$$

$$B_d(h) \approx \sum_{i=1}^{N} \frac{A^{i-1}B}{i!}\, h^i \tag{7}$$

However it is well known that the Taylor approximation is valid only for parameters near zero. As h is assumed to belong to the interval $[h_{min}, \quad h_{max}]$ with $h_{min} > 0$ the approximation will be considered around the nominal value h_0 of the sampling period, as:

$$h = h_0 + \delta \qquad \text{with} \qquad h_{min} - h_0 \leq \delta \leq h_{max} - h_0 \tag{8}$$

Then we get:

$$\begin{pmatrix} A_d & B_d \\ 0 & I \end{pmatrix} = \begin{pmatrix} A_{h_0} & B_{h_0} \\ 0 & I \end{pmatrix} \begin{pmatrix} A_\delta & B_\delta \\ 0 & I \end{pmatrix} \tag{9}$$

[1] the variable sampling period should be chosen in a range where the control performance is highly sensitive w.r.t. to the sampling rate, e.g. according to the rule of thumb $\omega_{cl}\, h \approx 0.2 \ldots 0.6$ where ω_{cl} is the desired closed-loop frequency [9]

where

$$\begin{pmatrix} A_{h_0} & B_{h_0} \\ 0 & I \end{pmatrix} = exp\left(\begin{pmatrix} A & B \\ 0 & 0 \end{pmatrix} h_0\right), \quad \begin{pmatrix} A_\delta & B_\delta \\ 0 & I \end{pmatrix} = exp\left(\begin{pmatrix} A & B \\ 0 & 0 \end{pmatrix} \delta\right)$$

This leads to

$$\begin{aligned} A_d &= A_{h_0} A_\delta \\ B_d &= B_{h_0} + A_{h_0} B_\delta \end{aligned} \tag{10}$$

Remark 1 *When $\delta = 0$, then $A_\delta = I$ and $B_\delta = 0$ which means that, as expected, $A_d = A_{h_0}$ and $B_d = B_{h_0}$.*

As h_0 is known at design time and constant, the Taylor approximation is then used only for A_δ and B_δ, as:

$$A_d(h) \approx A_{h_0}(I + \sum_{i=1}^{N} \frac{A^i}{i!}\ \delta^i) := A_d(\delta) \tag{11}$$

$$B_d(h) \approx B_{h_0} + A_{h_0}(\sum_{i=1}^{N} \frac{A^{i-1}B}{i!}\ \delta^i) := B_d(\delta) \tag{12}$$

To evaluate the approximation error due to the Taylor approximation, a criterion based on the H_∞ norm is chosen here to express the worst case error between G_{d_e} and G_d, both discrete-time models using respectively the exact method and the approximated one (i.e. the Taylor series approximation of order N).

$$J_N = \max_{h_{min}<h<h_{max}} \| G_{d_e}(h,z) - G_d(h,z) \|_\infty \tag{13}$$

2.2 A first polytopic model

As h belongs to the interval $[h_{min},\ h_{max}]$, then we can define $H = [\delta, \delta^2, \ldots, \delta^N]$ the vector of parameters. H belongs to a convex polytope (hyper-polygon) $\mathcal{H}$ (14) with 2^N vertices,.

$$\mathcal{H} = \left\{ \sum_{i=1}^{2^N} \alpha_i(\delta)\omega_i : \alpha_i(\delta) \geq 0, \sum_{i=1}^{2^N} \alpha_i(\delta) = 1 \right\} \tag{14}$$

$$\{\delta, \delta^2, \ldots, \delta^N\},\ \delta^i \in \{\delta^i_{min}, \delta^i_{max}\} \tag{15}$$

Each vertex is defined by a vector $\omega_i = [\nu_{i_1}, \nu_{i_2}, \ldots, \nu_{i_N}]$ where ν_{i_j} can take the extremum values $\{\delta^j_{min}, \delta^j_{max}\}$ with $\delta_{min} = h_{min} - h_0$ and $\delta_{max} = h_{max} - h_0$.

The matrices $A_d(\delta)$ and $B_d(\delta)$ are therefore affine in H and given by the polytopic forms:

$$A_d(H) = \sum_{i=1}^{2^N} \alpha_i(\delta) A_{d_i}, \quad B_d(H) = \sum_{i=1}^{2^N} \alpha_i(\delta) B_{d_i}$$

where the matrices at the vertices, i.e. A_{d_i} and B_{d_i}, are obtained by the calculation of $A_d(\delta)$ and $B_d(\delta)$ at each vertex of the polytope $\mathcal{H}$. The polytopic

coordinates α_i which represent the position of a particular parameter vector $H(\delta)$ in the polytope $\mathcal{H}$ are given solving :

$$H(\delta) = \sum_{i=1}^{2^N} \alpha_i(\delta)\omega_i \quad , \quad \alpha_i(\delta) \geq 0 \quad , \quad \sum_{i=1}^{2^N} \alpha_i(\delta) = 1 \tag{16}$$

As an illustration, figure 1 shows this transformation for $N = 2$ with

$$\begin{aligned} A_{d_1} &= A_d(H_1) \quad \text{or} \quad H_1 = [\delta_{min}, \delta^2_{min}] \\ A_{d_2} &= A_d(H_2) \quad \text{or} \quad H_2 = [\delta_{max}, \delta^2_{min}] \\ A_{d_3} &= A_d(H_3) \quad \text{or} \quad H_3 = [\delta_{min}, \delta^2_{max}] \\ A_{d_4} &= A_d(H_4) \quad \text{or} \quad H_4 = [\delta_{max}, \delta^2_{max}] \\ \mathcal{H} &= \mathbf{Co}\{H_1, H_2, H_3, H_4\} \end{aligned}$$

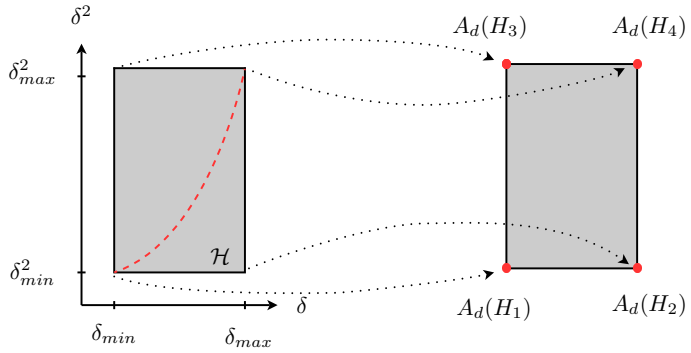

Figure 1: Example of polytope for $A_d(\delta)$ with $\delta_{min} = 0$

This leads to the plant polytopic model (17) where G_{d_i} are $G_d(H)$ evaluated at the vertices ω_i.

$$G_d(H) = \sum_{i=1}^{2^N} \alpha_i(\delta) G_{d_i} \quad \text{and} \quad H = \sum_{i=1}^{2^N} \alpha_i(\delta)\omega_i \tag{17}$$

As the gain-scheduled controller will be a convex combination of 2^N "vertex" controllers, the choice of the series order N gives a trade-off between the approximation accuracy and the controller complexity. Indeed one should notice that:

- The raw approach does not take into account the dependence between $\delta, \delta^2, \ldots, \delta^N$. Indeed, as shown in figure 1, the set of parameters $\{[\delta, \delta^2], 0 \leq \delta \leq \delta_{max}\}$, represented by the parabolic curve, is included in the large polytopic box with 4 vertices. This will of course induce some conservatism in the control design.
- Moreover, when a the order of the Taylor approximation increases, we will see (in section 4.1) that the number of LMIs to be solved, which is $2*2^N+1$ will grow exponentially which can lead to unfeasible optimisation problems.

- Finally the implementation of the controller is also directly linked to the number of vertices of the polytope.

To reduce the complexity (and the conservatism of the corresponding control design as well), a reduction of the polytope is proposed below.

Remark 2 *Note that exact calculations of matrix exponential via diagonalisation or Cayley-Hamilton theorems are more involved here as their expression will lead to non affine representations of $A_d(H)$ and $B_d(H)$.*

2.3 Reduction of the polytope

It is here proposed to reduce the size of the polytope using the dependency between the successive powers of the parameter δ. This reduction only stands for $\delta_{min} = 0$, which means that $h_0 = h_{min}$ is the minimal sampling period, i.e. related with a slack constraint on computing resource. For control purpose this choice is quite logical as the nominal behaviour corresponds to the minimal sampling period in normal situations. This period would increase only when computing resources will be limited.

The way to reduce the size of the polytopic set can be seen on the example in figure 1, where the parabolic parameters locus is enclosed in the triangle defined by $\{0,0\}$, $\{\delta_{max},0\}$ and $\{\delta_{max},\delta_{max}^2\}$. Therefore it is not necessary to consider the vertex $\{0,\delta_{max}^2\}$ to build a polytope encompassing the parameters locus.

To develop and extend this method to a polytope of size N, let us write:

$$h = h_{min} + \delta, \quad 0 \leq \delta \leq \delta_{max}, \quad \delta_{max} = h_{max} - h_{min}, \tag{18}$$

Then the inequality below is always satisfied:

$$\delta\ \delta^n \leq \frac{\delta_{max}^{n+1}}{\delta_{max}^n}\ \delta^n \quad \text{i.e.} \quad \delta^{n+1} \leq \delta_{max}\ \delta^n \tag{19}$$

Then it is proposed to delete the vertices which do not satisfy the above inequality. As the vertices H_i of $\mathcal{H}$ are given by a vector $(\nu_1, \nu_2, \ldots, \nu_N)$ where $\nu_i = 0$ or δ_{max}^i according to the considered vertex, then the inequality to be satisfied is given by:

$$\nu_{n+1} \leq \delta_{max}\ \nu_n \tag{20}$$

This leads to the following set of admissible vertices:

$$\begin{aligned}
&(0,0,0,\ldots,0)\\
&(\delta_{max},0,0,\ldots,0)\\
&(\delta_{max},\delta_{max}^2,0,\ldots,0)\\
&\vdots\\
&(\delta_{max},\delta_{max}^2,\delta_{max}^3,\ldots,\delta_{max}^N)
\end{aligned} \tag{21}$$

Remark 3 *The vertex $(0,\delta_{max}^2,0,\ldots,0)$ does not satisfy inequality (20) and can be discarded.*

This method leads to a set of $N+1$ vertices instead of 2^N. Note that these vertices are linearly independent and make a simplex, which is itself basically a polytope [10] of minimal dimension considering the parameters space of dimension N.

When $N = 2$ (and for $0 < \delta < \delta_{max}$) the square is downsized to the triangle in figure 2. When $N = 3$ the pyramid in figure 3 is the reduction of a cube.

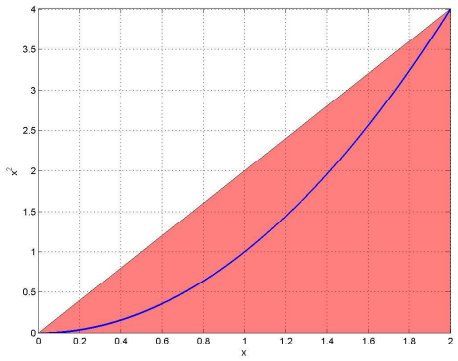

Figure 2: Polytope reduction for N=2

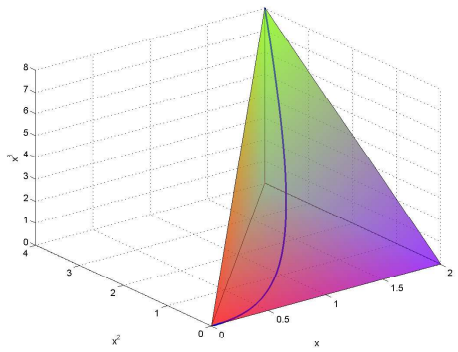

Figure 3: Polytope reduction for N=3

3 Formulation of the H_∞/LPV control problem

In this section we first present the formulation of the H_∞ control problem using weighting function depending on the sampling period. Indeed the provided methodology will allow for performance adaptation according to the computing resources availability.

The H_∞ framework is based on the general control configuration of figure 4, where W_i and W_o are some weighting functions representing the specification of the desired closed-loop performances (see [11]). The objective is here to find a controller K such internal stability is achieved and $\|\tilde{z}\|_2 < \gamma\|\tilde{w}\|_2$, where γ represents the H_∞ attenuation level.

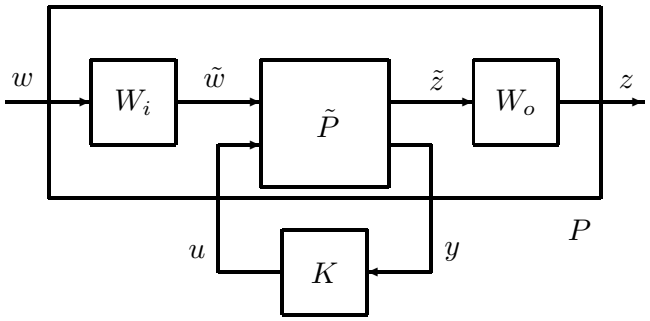

Figure 4: Focused interconnection

3.1 Towards discrete-time weighting functions

Classical control design assumes constant performance objectives and produces a controller with an unique sampling period. The sampling period is chosen according to the controller bandwidth, the noise sensibility and the availability of computation resources. When the sampling period varies the usable controller bandwidth also varies and the closed-loop objectives should logically be adapted. Therefore we propose to adapt the bandwidth of the weighting functions to the sampling period.

The methodology is as follows. First W_i and W_o are split into two parts :

- a constant part with constant poles and zeros. This allows, for instance, to compensate for oscillations or flexible modes which are, by definition, independent of the sampling period.
- the variable part contains poles and zeros whose pulsations are expressed as an affine function of the sampling frequency $f = 1/h$. This allows for an adaption of the bandwidth of the weighting functions, and hence for an adaption of the closed-loop performance w.r.t. the available computing power. These poles and zeros are here constrained to be *real* by the discretization step.

First of all the constant parts of the weighting functions are merged with the continuous-time plant model. Then a discrete-time augmented system is developed as presented above.

The variable part $V(s)$ of a weighting function is the discretized according to the following methodology:

1. factorise $V(s)$ as a product of first order systems. We here chose poles and zeros depending linearly of the sampling frequency $f = 1/h$, as:

$$V(s) = \beta \prod_i \frac{s - b_i f}{s - a_i f} = \beta \prod_i V_i(s) \tag{22}$$

   with $a_i, b_i \in \mathbb{R}$

2. Consider the state space observable canonical form for $V_i(s)$

$$V_i(s) : \begin{cases} \dot{x}_i = a_i f \; x_i + f(a_i - b_i) \; u_i \\ y_i = x_i + u_i \end{cases} \tag{23}$$

3. form the series interconnection of the state space representation of each $V_i(s)$. This allows to get $V(s)$ of the form (24) with appropriate dimensions of the state space matrices.

$$V(s): \left\{ \begin{array}{rcl} \dot{x}_v & = & A_v f\ x_v + B_v f\ u_v \\ y_v & = & C_v\ x_v + D_v\ u_v \end{array} \right. \tag{24}$$

4. Get the discrete-time state space representation of $V(s)$. Thanks to the affine dependence in f in (24) the discrete-time model of the variable part becomes independent of h since:

$$\left\{ \begin{array}{l} A_{v_d} = e^{A_v f\ h} = e^{A_v} \\ B_{v_d} = (A_v f)^{-1}(A_{v_d} - I)B_v f = (A_v)^{-1}(A_{v_d} - I)B_v \\ C_{v_d} = C_v \text{ and } D_{v_d} = D_v \end{array} \right. \tag{25}$$

Remark 4 *The serial interconnection of two systems of the form* (26) *leads to a system of the form* (27).

$$\left\{ \begin{array}{l} \dot{x} = Af\ x + Bf\ u \\ y = C\ x + D\ u \end{array} \right. \tag{26}$$

$$\begin{array}{lll} A = \begin{pmatrix} A_1 & 0 \\ B_2C_1 & A_2 \end{pmatrix} & B = \begin{pmatrix} B_1 \\ B_2D_1 \end{pmatrix} & x = \begin{pmatrix} x_1 \\ x_2 \end{pmatrix} \\ C = \begin{pmatrix} D_2C_1 & C_2 \end{pmatrix} & D = D_2D_1 & \end{array} \tag{27}$$

As seen matrices C and D only depend on C_i or D_i, $i = 1, 2$, which ensures that they do not depend on f. Then there is no coupling between A_i and B_i, $i = 1, 2$, which keeps the linear dependence on f of the state space equation. As illustration and forward, the interconnection of 3 systems leads to a state space representation (28) *:*

$$\begin{array}{lll} A = \begin{pmatrix} A_1 & 0 & 0 \\ B_2C_1 & A_2 & 0 \\ B_3D_2C_1 & B_3C_2 & A_3 \end{pmatrix} & B = \begin{pmatrix} B_1 \\ B_2D_1 \\ B_3D_2D_1 \end{pmatrix} & x = \begin{pmatrix} x_1 \\ x_2 \\ x_3 \end{pmatrix} \\ C = \begin{pmatrix} D_3D_2C_1 & D_3C_2 & C_3 \end{pmatrix} & D = D_3D_2D_1 & \end{array} \tag{28}$$

By iteration, the serial interconnection of more than three systems (26) *still keeps the form* (26). *Therefore the interconnection of systems $V_i(p)$ which are in form* (26) *leads to a system in the form* (24) *where the dependence on f makes easier the discretization step.*

Remark 5 *The simplification between f and h in* (25) *makes easy the discretization step. This is why the plant and the weighting functions are separately discretized, and the augmented plant is obtained in discrete time afterwards by interconnection. This is also a consequence of the use of the observable canonical form.*

3.2 The discrete-time augmented plant

Let us here present the overall methodology to get the discrete-time plant interconnection.

Let first consider the following continuous-time model where the constant part of the weighting function W_i and W_o has been connected to the plant model:

$$P : \begin{cases} \dot{x}(t) = Ax(t) + B_w w(t) + B_u u(t) \\ z(t) = C_z x(t) + D_{zw} w(t) + D_{zu} u(t) \\ y(t) = C_y x(t) + D_{yw} w(t) + D_{yu} u(t) \end{cases} \tag{29}$$

where $x \in R^n$ is the state, $w \in R^{m_w}$ represents the exogenous inputs, $u \in R^{m_u}$ the control inputs, $z \in R^{p_z}$ the controlled output and $y \in R^{p_y}$ the measurement vector.

A discrete-time representation of the above system is first obtained thanks to the previous methodology. For simplicity we will note, according to the representation (1):

$$A = A \qquad B = \begin{pmatrix} B_w & B_u \end{pmatrix} \qquad C = \begin{pmatrix} C_z \\ C_y \end{pmatrix} \qquad D = \begin{pmatrix} D_{zw} & D_{zu} \\ D_{yw} & D_{yu} \end{pmatrix} \tag{30}$$

Using the Taylor approximation at order N leads to a polytope $\mathcal{H}$. This polytope has r vertices (where r equals 2^N for the basic case and $N+1$ for the reduced one). Each of the r vertices is described by a vector ω_i of the form $(\delta_1, \delta_2, \ldots, \delta_r)$ where $\delta_i = \delta^i_{min}$ or δ^i_{max}.

The LPV polytopic discrete-time model is given by:

$$\mathcal{P}(H) : \begin{cases} x_{k+1} = \mathcal{A}(H)x_k + \mathcal{B}_w(H)w + \mathcal{B}_u(H)u \\ z = C_z x_k + D_{zw} w + D_{zu} u \\ y = C_y x_k + D_{yw} w + D_{yu} u \end{cases} \tag{31}$$

$$\begin{gathered} H = \begin{pmatrix} \delta & \delta^2 & \ldots & \delta^N \end{pmatrix} \qquad H \in \mathcal{H} = \mathbf{Co}\{\omega_1, \ldots, \omega_r\} \\ H = \sum_{i=1}^{r} \alpha_i \omega_i \qquad \mathcal{A}(H) = \sum_{i=1}^{r} \alpha_i \mathcal{A}_i \qquad \sum_{i=1}^{r} \alpha_i = 1 \qquad \alpha_i \geq 0 \end{gathered} \tag{32}$$

where, according to the representation (2)

$$A_d = \mathcal{A} \qquad B_d = \begin{pmatrix} \mathcal{B}_w & \mathcal{B}_u \end{pmatrix} \qquad C_d = C \qquad D_d = D \tag{33}$$

Now, the variable part of the weighting functions W_i and W_o are expressed as previously presented, which leads to both discrete-time representations (34) and(35) where the size of the state vector depend on the weighting function:

$$\mathcal{W}_I : \begin{cases} x_{I_{k+1}} = A_I x_{I_k} + B_I \tilde{w} \\ w = C_I x_{I_k} + D_I \tilde{w} \end{cases} \tag{34}$$

$$\mathcal{W}_O : \begin{cases} x_{O_{k+1}} = A_O x_{O_k} + B_O z \\ \tilde{z} = C_O x_{O_k} + D_O z \end{cases} \tag{35}$$

The augmented system $\mathcal{P}'(H)$ is obtained by the interconnection of $\mathcal{P}(H)$, $\mathcal{W}_I$ and $\mathcal{W}_O$. Therefore we obtain the following LPV polytopic discrete-time system of state vector $x'_k = (x_k \ x_{I_k} \ x_{O_k})^T$:

$$\mathcal{P}'(H): \begin{cases} x'_{k+1} = \mathcal{A}'(H)x'_k + \mathcal{B}'_w(H)\tilde{w} + \mathcal{B}'_u(H)u \\ \tilde{z} = \mathcal{C}'_z x'_k + \mathcal{D}'_{zw}\tilde{w} + \mathcal{D}'_{zu}u \\ y = \mathcal{C}'_y x'_k + \mathcal{D}'_{yw}\tilde{w} + \mathcal{D}'_{yu}u \end{cases} \tag{36}$$

with

$$\mathcal{A}'(H) = \begin{pmatrix} \mathcal{A}(H) & \mathcal{B}_w(H)C_I & 0 \\ 0 & A_I & 0 \\ B_O C_z & B_O D_{zw} C_I & A_O \end{pmatrix} \quad \mathcal{B}'_w(H) = \begin{pmatrix} \mathcal{B}_w(H)D_I \\ B_I \\ B_O D_{zw} D_I \end{pmatrix} \quad \mathcal{B}'_u(H) = \begin{pmatrix} \mathcal{B}_u(H) \\ 0 \\ B_O D_{zu} \end{pmatrix}$$

$$\mathcal{C}'_z = \begin{pmatrix} D_O C_z & D_O D_{zw} C_I & C_O \end{pmatrix} \quad \mathcal{D}'_{zw} = \begin{pmatrix} D_O D_{zw} D_I \end{pmatrix} \quad \mathcal{D}'_{zu} = \begin{pmatrix} D_O D_{zu} \end{pmatrix}$$

$$\mathcal{C}'_y = \begin{pmatrix} C_y & D_{yw} C_I & 0 \end{pmatrix} \quad \mathcal{D}'_{yw} = \begin{pmatrix} D_{yw} D_I \end{pmatrix} \quad \mathcal{D}'_{yu} = \begin{pmatrix} D_{yu} \end{pmatrix}$$

4 Solution to the H_∞ control problem for LPV systems

We aim to use here the H_∞ control design for linear parameter-varying systems as stated in [7]. Let the discrete-time LPV plant, mapping exogenous inputs w and control inputs u to controlled outputs z and measured outputs y, with $x \in \mathbb{R}^{n_x}$, be given by the polytopic model:

$$\begin{cases} x_{k+1} = \mathcal{A}'(H)x_k + \mathcal{B}'_w(H)w + \mathcal{B}'_u(H)u \\ z = \mathcal{C}'_z x_k + \mathcal{D}'_{zw}w + \mathcal{D}'_{zu}u \\ y = \mathcal{C}'_y x_k + \mathcal{D}'_{yw}w + \mathcal{D}'_{yu}u \end{cases} \tag{37}$$

where the dependence of the state space matrices on H is affine and the parameter vector H, ranges over a fixed polytope $\mathcal{H}$ with r vertices ω_i

$$\mathcal{H} = \left\{ \sum_{i=1}^{r} \alpha_i(\delta)\omega_i : \alpha_i(\delta) \geq 0, \sum_{i=1}^{r} \alpha_i(\delta) = 1 \right\} \tag{38}$$

where r is equal to $N+1$ or to 2^N according to the kind of polytope (reduced or full).

4.1 Problem resolvability

The method considered here requires the following assumptions:

(A1) $\mathcal{D}'_{yu}(H) = 0$

(A2) $\mathcal{B}'_u(H), \mathcal{C}'_y, \mathcal{D}'_{zu}, \mathcal{D}'_{yw}$ are parameter- independent

(A3) the pairs $(\mathcal{A}'(H), \mathcal{B}'_u(H))$ and $(\mathcal{A}'(H), \mathcal{C}'_y)$ are quadratically stabilisable and detectable over H respectively,

Remark 6 *In* (37) *assumption (A2) is not satisfied due to the* $B_u(H)$ *term in* $\mathcal{B}'_u(H)$*. To avoid this, a strictly proper filter is added on the control input, as explained in [12, 13]. It is a numerical artifact (which of course increases the number of state variables* $n_e > n_x$*), therefore its bandwidth should be chosen high enough to be negligible regarding the plant and objective bandwidths.*

Proposition 1 *Following [7] , under the previous assumptions there exists a gain-scheduled controller (Figure 5)*

$$\left\{ \begin{array}{rcl} x_{K_{k+1}} & = & A_K(H)x_{K_k} + B_K(H)y_k \\ u_k & = & C_K(H)x_{K_k} + D_K(H)y_k \end{array} \right. \tag{39}$$

where $x_K \in \mathbb{R}^{n_e}$, which ensures, over all parameter trajectories, that :

- *the closed-loop system is internally quadratic stable;*
- *the $\mathscr{L}_2$-induced norm of the operator mapping w into z is bounded by γ, i.e. $\|z\|_2 < \gamma\|w\|_2$*

if and only if there exist γ and two symmetric matrices (R, S) satisfying $2r+1$ LMIs (which are computed off-line) :

$$\left(\begin{array}{c|c} N_R & 0 \\ \hline 0 & I \end{array}\right)^T \mathcal{L}_1 \left(\begin{array}{c|c} N_R & 0 \\ \hline 0 & I \end{array}\right) < 0, i = 1 \ldots r \tag{40}$$

$$\left(\begin{array}{c|c} N_S & 0 \\ \hline 0 & I \end{array}\right)^T \mathcal{L}_2 \left(\begin{array}{c|c} N_S & 0 \\ \hline 0 & I \end{array}\right) < 0, i = 1 \ldots r \tag{41}$$

$$\left(\begin{array}{cc} R & I \\ I & S \end{array} \right) \geq 0 \tag{42}$$

where

$$\mathcal{L}_1 = \left(\begin{array}{cc|c} \bar{A}_i R \bar{A}_i^T - R & \bar{A}_i R C_{1i}^T & \bar{B}_{1i} \\ \bar{C}_{1i} R \bar{A}_i^T & -\gamma I + \bar{C}_{1i} R \bar{C}_{1i}^T & \bar{D}_{11i} \\ \hline \bar{B}_{1i}^T & D_{11i}^T & -\gamma I \end{array}\right)$$

$$\mathcal{L}_2 = \left(\begin{array}{cc|c} \bar{A}_i^T S \bar{A}_i - S & \bar{A}_i^T S \bar{B}_{1i} & \bar{C}_{1i}^T \\ \bar{B}_{1i}^T S \bar{A}_i & -\gamma I + B_{1i}^T S \bar{B}_{1i} & \bar{D}_{11i}^T \\ \hline C_{1i} & D_{11i} & -\gamma I \end{array}\right)$$

where $\bar{A}_i$, $\bar{B}_{1i}$, $\bar{C}_{1i}$, $\bar{D}_{11i}$ are $\bar{A}(H)$, $\mathcal{B}'_w(H)$, $\mathcal{C}'_z(H)$, $\mathcal{D}'_{zw}(H)$ evaluated at the i^{th} vertex of the parameter polytope. N_S and N_R denote bases of null spaces of $(\bar{B}_2^T, \bar{D}_{12}^T)$ and $(\bar{C}_2, \bar{D}_{21})$ respectively.

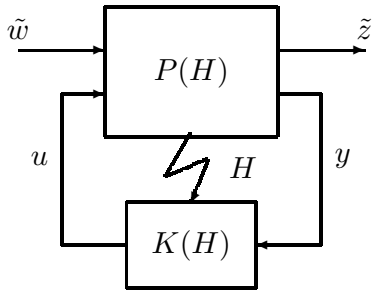

Figure 5: Closed-loop of the LPV system

4.2 Controller reconstruction

Once R, S and γ are obtained, the controllers are reconstructed at each vertex of the parameter polytope as shown in [12]. The gain-scheduled controller $K(H)$ is then the convex combination of these controllers

$$K(H) : \begin{pmatrix} A_K(H) & B_K(H) \\ C_K(H) & D_K(H) \end{pmatrix} = \sum_{i=1}^{r} \alpha_i(\delta) \begin{pmatrix} A_{K_i} & B_{K_i} \\ C_{K_i} & D_{K_i} \end{pmatrix} \tag{43}$$

$$\text{with } \alpha_i(\delta) \text{ such that } H = \sum_{i=1}^{r} \alpha_i(\delta)\omega_i \tag{44}$$

Note that on-line scheduling of the controller needs the computation of $\alpha_i(\delta)$ knowing h. For the full polytope case the polytopic coordinates are solutions of the following under-constrained system ([14, 15]) :

$$\begin{cases} \sum_{i=1}^{2^N} \alpha_i(\delta)\omega_i = H = [\delta, \delta^2, ..., \delta^N] \\ \sum_{i=1}^{2^N} \alpha_i(\delta) = 1, \ \alpha_i(\delta) \geq 0 \end{cases} \tag{45}$$

which can be solved using an algorithm of the LMI toolbox [16]. When the polytope is reduced to a simplex (using inequality (20)) the polytopic coordinates are given solving a simpler system :

$$\begin{cases} \sum_{i=1}^{N+1} \alpha_i(\delta)\omega_i = H = [\delta, \delta^2, ..., \delta^N] \\ \sum_{i=1}^{N+1} \alpha_i(\delta) = 1, \ \alpha_i(\delta) \geq 0 \end{cases} \tag{46}$$

for which explicit solutions are easily recursively computed:

$$\begin{cases} \alpha_1 = \frac{\delta_{max} - \delta}{\delta_{max} - \delta_{min}} \\ \alpha_n = \frac{\delta^n_{max} - \delta^n}{\delta^n_{max} - \delta^n_{min}} - \sum_1^{n-1} \alpha_i \quad , \quad n = [2, ..., N] \\ \alpha_{N+1} = 1 - \sum_1^N \alpha_i \end{cases} \tag{47}$$

This leads, for the case $N = 2$ and $\delta_{min} = 0$ of the next section to the simple explicit solutions:

$$\alpha_1 = \frac{\delta_{max} - \delta}{\delta_{max}}, \alpha_2 = \frac{\delta^2_{max} - \delta^2}{\delta^2_{max}} - \alpha_1, \alpha_3 = 1 - (\alpha_1 + \alpha_2)$$

5 Control of the T inverted pendulum

This section is devoted to an experimental validation of the approach using a "T" inverted pendulum of Educational Control Products[2], available at GIPSA-lab, in the NeCS (Network Controlled Systems) team. These experiments will emphasise the effectiveness of the proposed design method.

[2] `http://www.ecpsystems.com/controls_pendulum.htm`

5.1 System description

The pendulum shown in figures 6 and 7 is made of two rods. A vertical one which rotates around the pivot axle, and an horizontal sliding balance one. Two optional masses allow to modify the plant's dynamical behaviour.

The control actuator (DC motor) delivers a force u to the horizontal sliding rod, through a drive gear-rack.

The θ angle, positive in the trigonometric sense, is measured by the rod angle sensor. The position z of the horizontal rod is measured by a sensor located at the motor axle.

The DC motor is torque controlled using a local current feedback loop (assumed to be a simple gain due to its fast dynamics). The dynamical behaviour of the sensors is also neglected.

Figure 6: Picture of the T pendulum

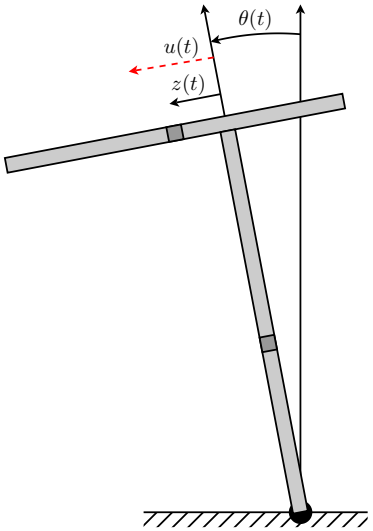

Figure 7: Coordinates of the T pendulum

5.2 Modelling

A mechanical model of the pendulum is presented below, which takes into account the viscous friction (but not the Coulomb friction).

$$\begin{pmatrix} m_1 & m_1 l_0 \\ m_1 l_0 & \bar{J} \end{pmatrix} \begin{pmatrix} \ddot{z} \\ \ddot{\theta} \end{pmatrix} + \begin{pmatrix} -f_{v_z} & -m_1 z\dot{\theta} \\ 2m_1 z\dot{\theta} & 0 \end{pmatrix} \begin{pmatrix} \dot{z} \\ \dot{\theta} \end{pmatrix} + \begin{pmatrix} -m_1 \sin\theta \\ -(m_1 l_0 + m_2 l_c)\sin\theta - m_1 z\cos\theta \end{pmatrix} g = \begin{pmatrix} u \\ 0 \end{pmatrix} \quad (48)$$

where the time dependence of the state variables is implicit, and the parameter values of given below in table 1.

Table 1: Parameters

Name	Value	Description
m_1	0.217 kg	horizontal sliding rod mass
m_2	1.795 kg	vertical rod mass
l_0	0.33	vertical rod length
l_c	-0.032 m	vertical rod position of the centre of gravity
g	9.81 m.s^{-2}	gravity acceleration
$\bar{J}$	0.061 Nm^2	Nominal inertia
f_{v_z}	0.1 kg.s^{-1}	viscous friction

Choosing the state vector as $x = [z, \dot{z}, \theta, \dot{\theta}]$, we get the following non linear state space representation:

$$\begin{cases} \dot{x}_1 = x_2 \\ \dot{x}_2 = -l_0\dot{x}_4 + x_1x_4^2 + g\sin x_3 - \dfrac{f_{v_z}}{m_1}x_2 + \dfrac{u}{m_1} \\ \dot{x}_3 = x_4 \\ \dot{x}_4 = \dfrac{1}{J_0(x_1) - m_1l_0^2}\,(+g(m_1x_1\cos x_3 + m_2l_c\sin x_3) \\ \qquad -m_1(l_0x_4 + 2x_2)x_1x_4 - l_0u) \end{cases} \tag{49}$$

with $J_0(x_1) = \bar{J} + m_1x_1^2$. The steady-state linearisation around $x = [0, 0, 0, 0]$ gives the linear state space representation $\dot{x}(t) = Ax(t) + Bu(t)$, $y(t) = Cx(t)$ with

$$A = \begin{pmatrix} 0 & 1 & 0 & 0 \\ \frac{-l_0gm_1}{\bar{J}-m_1l_0^2} & -\frac{f_{v_z}}{m_1} & \frac{-l_0gm_2l_c}{\bar{J}-m_1l_0^2} + g & 0 \\ 0 & 0 & 0 & 1 \\ \frac{gm_1}{\bar{J}-m_1l_0} & 0 & \frac{gm_2l_c}{\bar{J}-m_1l_0^2} & 0 \end{pmatrix}, B = \begin{pmatrix} 0 \\ \frac{l_0^2}{\bar{J}-m_1l_0^2} + \frac{1}{m_1} \\ 0 \\ \frac{-l_0}{\bar{J}-m_1l_0^2} \end{pmatrix}$$

$$C = \begin{pmatrix} 1 & 0 & 0 & 0 \\ 0 & 0 & 1 & 0 \end{pmatrix}$$

which gives numerically:

$$A = \begin{pmatrix} 0 & 1 & 0 & 0 \\ -18.79 & -0.46 & 14.82 & 0 \\ 0 & 0 & 0 & 1 \\ 56.92 & 0 & -15.18 & 0 \end{pmatrix} \quad B = \begin{pmatrix} 0 \\ 7.52 \\ 0 \\ -8.82 \end{pmatrix} \tag{50}$$

The poles of the linear model are $p_{1,2} = -0.122 \pm 6.784$, $p_3 = -3.592$ and $p_4 = 3.376$.

5.3 Performance specification

As such a T pendulum system is difficult to be controlled, our main objective is here to get a closed-loop stable system, to emphasise the practical feasibility of the proposed methodology for real-time control.

From previous experiments with this plant the sampling period is assumed to be in the interval $[1, 3]$ ms.

The chosen performance objectives are represented in figure 8, where the tracking error and the control input are weighted (as usual in the H_∞ methodology).

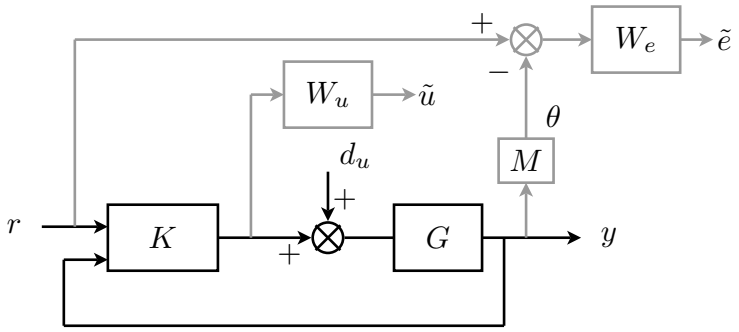

Figure 8: General control configuration

This corresponds to the simple mixed sensitivity problem given in (51).

$$\left\| \begin{matrix} W_e(I - MS_yGK_1) & W_eMS_yG \\ W_uS_uK_1 & W_uT_u \end{matrix} \right\|_\infty \leq \gamma \tag{51}$$

with

$$\begin{aligned} K &= \begin{bmatrix} K_1 & K_2 \end{bmatrix} & M &= \begin{bmatrix} 0 & 0 & 1 & 0 \end{bmatrix} \\ S_u &= (I - K_2G)^{-1} & S_y &= (I - GK_2)^{-1} \\ T_u &= -K_2G(I - K_2G)^{-1} \end{aligned} \tag{52}$$

The performance objectives are represented by weighting functions and may be given by the usual transfer functions [11]:

$$W_e(p, f) = \frac{p\, M_S + \omega_S(f)}{p + \omega_S\, \epsilon_S} \qquad \omega_S(f) = h_{min}\, \omega_{S_{max}}\, f \tag{53}$$

$$W_u(p, f) = \frac{1}{M_U} \tag{54}$$

where $f = 1/h$, $\omega_{S_{max}} = 1{,}5$ rad/s, $M_S = 2$, $\epsilon_S = 0.01$ and $M_U = 5$.

Notice that only W_e depends on the sampling frequency to account for performance adaptation.

5.4 Polytopic discrete-time model

We follow here the methodology proposed in section 2. The approximation is done around the nominal period $h_o = 1ms$, for $h \in [1, 3]$ ms, i.e. $\delta_h \in [0, 2]$ ms (see Remark 2).

On figure 9 the criterion (13) is evaluated for different sampling periods ($h \in [1, 3]ms$) and different orders of the Taylor expansions ($k \in [1, 5]$). It shows that this error may be large only if the order 1 is used.

On figure 10 $|G_{d_e}(\delta_h, z) - G_d(\delta_h, z)|$ is plotted according to the frequency, evaluated for 5 sampling periods (i.e. $\delta_h \in [0, 2]ms$) and for two cases of Taylor expansions (2 and 4). This allows to conclude that the choice of an order 2 of the Taylor expansion is already quite good as it leads to an approximation error less than $-40dB$ in the selected sampling frequency interval. Note that choosing the case "order 2" leads to a reduced polytope with 3 vertices.

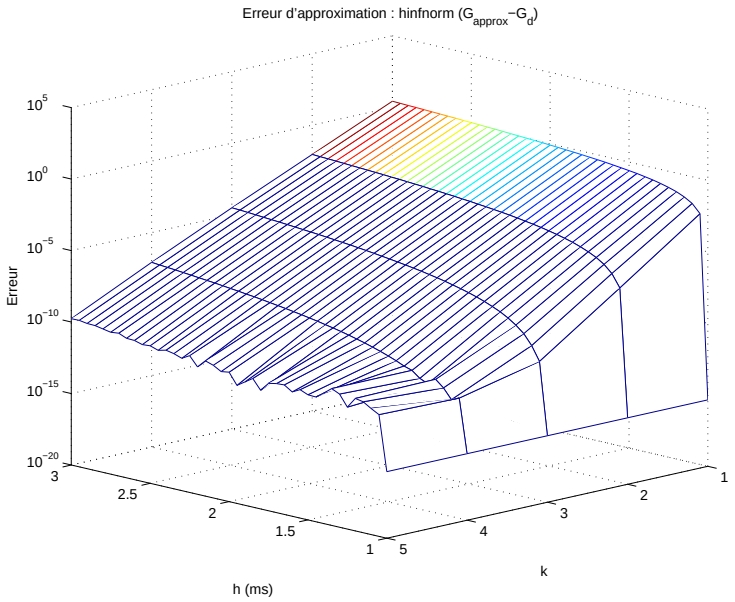

Figure 9: Approximation error

5.5 LPV/H_∞ design

The first step is the discretization of the weighting functions. The augmented system is got, using a preliminary first-order filtering of the control input, to satisfy the design assumptions. The augmented system is of order 6.
Applying the design method developed in section 4 leads to the following results, combining the Taylor expansion order and the polytope reduction:

	Polytope	Nb vertices	γ_{opt}
Taylor order N=2	full	4	1.1304
Taylor order N=2	reduced	3	1.1299
Taylor order N=4	full	16	1.1313
Taylor order N=4	reduced	5	1.1303

This table emphasises that both design of orders 2 and 4 are reliable. For implementation reasons (simplicity and computational complexity) we have chosen the case of the reduced polytope using a Taylor expansion of order 2.

The corresponding sensitivity functions of the chosen design are shown in figure 11. Using $S_e = e/r$ the steady-state tracking error is less than $-46dB$, with a varying bandwidth from 0.4 to 1.2 rad/s, i.e the ratio 3, specified according to the interval of sampling period, is satisfied.

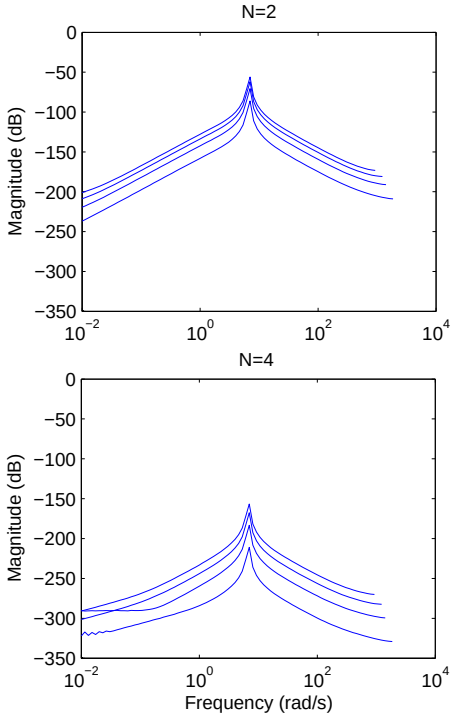

Figure 10: $|G_{d_e}(\delta_h, z) - G_d(\delta_h, z)|$ for $\neq h$ - Taylor order 2 and 4

The peak value of $S_u K_1$ varies from 1.2 to $10.8dB$, which is reasonable for the control gain. Note that in this particular case study we will benefit from the relatively high sensitivity in high frequencies, as it allows some persistent dithering in the control action and reduces the effect of friction, as we will see in the experiments.

Finally the function $MS_y Gd_u$ is very low so that the effect of input disturbance d_u on the tracking error will be greatly attenuated.

Figure 12 shows the time-domain response of the non linear pendulum model (angle and position) interconnected with the discrete-time LPV sampling variable controller (here for different frozen values of the sampling periods). The settling time varies from 1.1 to 4.8 sec, i.e. in a ratio 4.3. Indeed we observe here the graceful and controlled degradation of the performance due to the adaption of the sampling dependent weighting functions. There is no overshoot, as expected from the frequency responses of the sensitivity function $S_y G K_1$.

5.6 Simulation results

In this section, the application of the proposed sampling variable controller when the sampling period varies on-line between 1 and 3 msec. is provided.

Two cases are presented. First in figure 13 the sampling period variation is continuous and follows a sinusoidal signal of frequency $0.15rad/s$. Then in figure 14 some step changes of the sampling period are done.

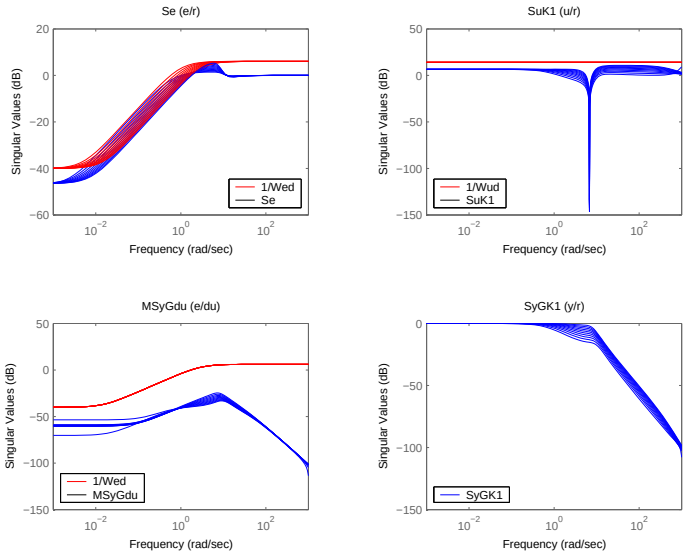

Figure 11: Sensitivity functions

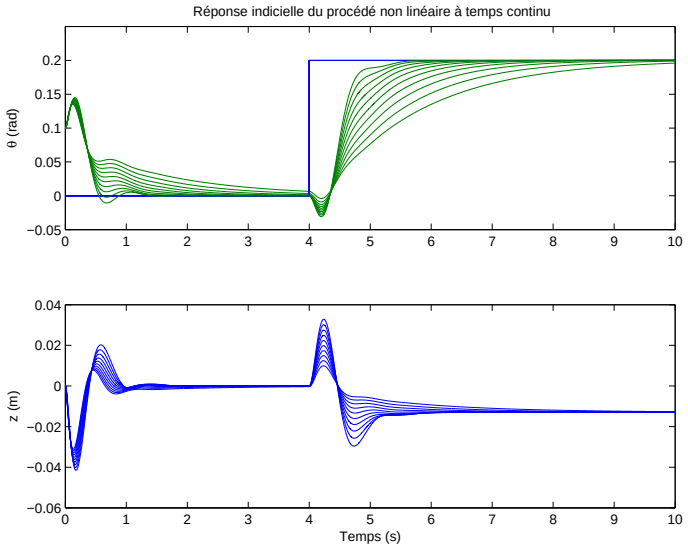

Figure 12: Response time of the continuous time non-linear process

These results show that, as expected from the performance specification, the settling time of the closed-loop system varies accordingly with the sampling period. When the period is large (i.e at $t = 10sec$) the pendulum is slower, while when the period is small (i.e at $t = 30sec$ in Fig. 13) the pendulum response is faster. Moreover, thanks to the LPV approach, the variations (sinusoidal or step changes) of the sampling period do not lead to abrupt transient of the pendulum behaviour. This is a great benefit from the LPV approach which ensures the stability for arbitrarily fast variations of the parameter in their allowed range

(this is due to the use of a single Lyapunov function in the design [7]). The same assessment can be done for the control input.

The LPV scheme allows here to guarantee the closed-loop quadratic stability, to have a bounded $\mathscr{L}_2$-induced norm for all variation of the sampling period and to have a predictable closed-loop behaviour.

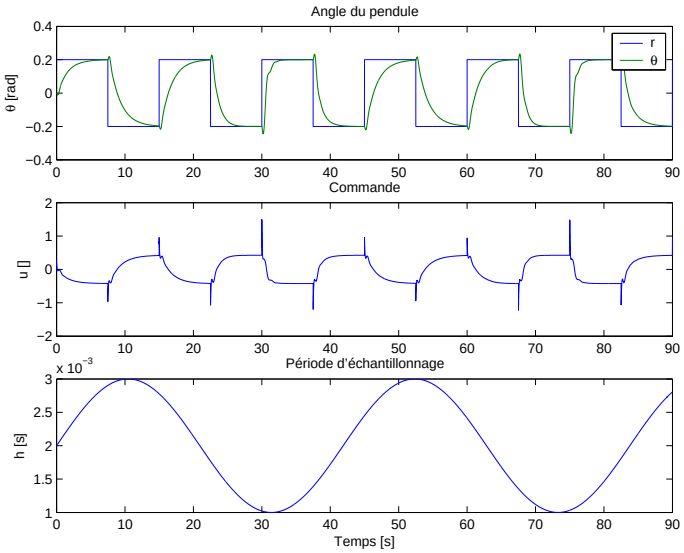

Figure 13: Motion of the T pendulum under a sinusoidal sampling period

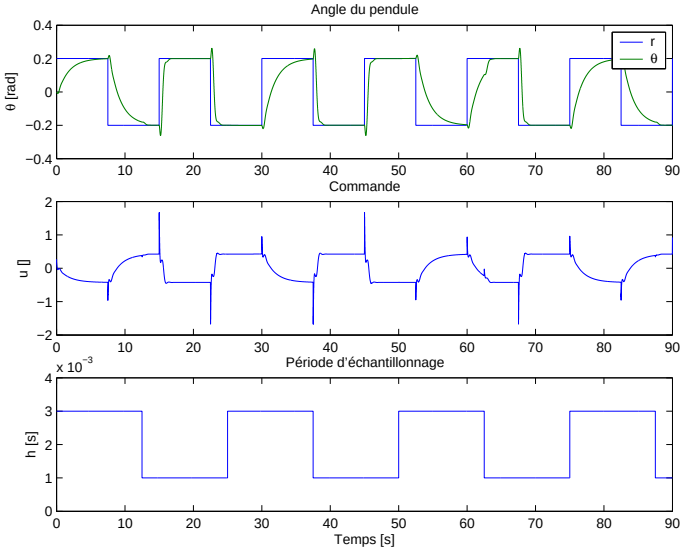

Figure 14: Motion of the T pendulum under a square sampling period

5.7 Experiments

The scenarii of the previous section (simulation results) are now implemented for the real plant of figure 6. The plant is controlled through Matlab/Simulink using the Real-time Workshop and xPC Target.

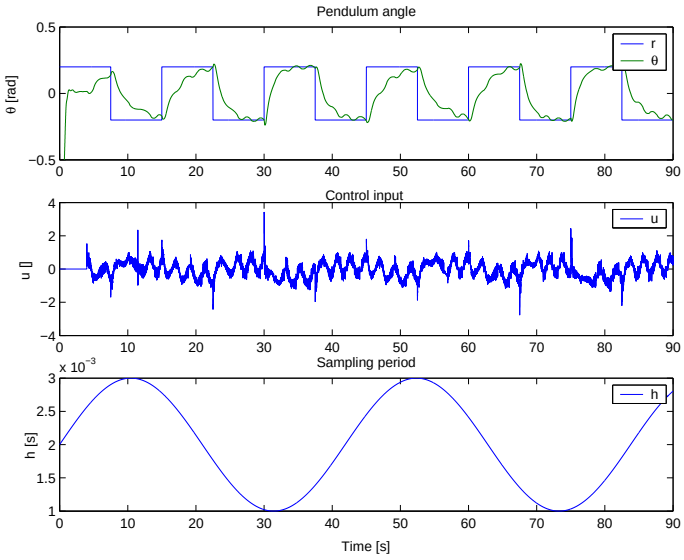

Figure 15: Experimental motion of the T pendulum under a sinusoidal sampling period

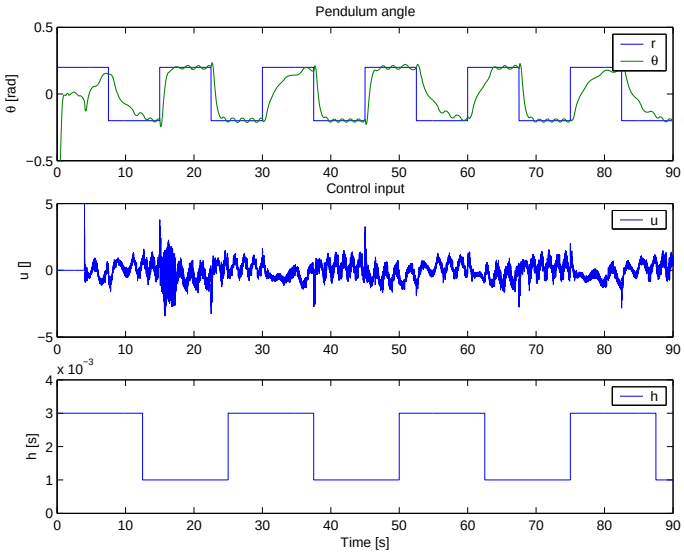

Figure 16: Experimental motion of the T pendulum under a square sampling period

The results are given in figures 15 and 16. As in the previous section, the settling time is maximal when the sampling period is maximal, and conversely. In the same way, there is no abrupt changes in the control input (even when the sampling period abruptly varies from 1 to 3 ms as in figure 16).

Note that, as explained before, the real control input is sensitive to noise, allowing to minimise the friction effect, and therefore to obtain a closed-loop system with much less oscillations.

Finally we get similar results in simulation and experimental tests which shows the inherent robustness property of the H_∞ design.

These results emphasise the great advantage and flexibility of the method when the available computing resources may vary, and when sampling period variations are used to handle computing flexibility such as in [4].

6 Conclusion

In this paper, an LPV approach is proposed to design a discrete-time linear controller with a varying sampling period and varying performances. A way to reduce the polytope from 2^N to $N+1$ vertices (where N is the Taylor order expansion) is provided, which drastically reduces both the conservatism and the complexity of the resulting sampling dependent controller and makes the solution easier to implement. Further developments may concern the reduction of the conservatism which is due to to the use a constant Lyapunov function approach, which is known to produce a sub-optimal controller. Another approach based on [17] is presented in [13] but up to now did not give improvements in the results.

Also the complete methodology has been implemented for the case of a "T" inverted pendulum, where experimental results have been provided. These results emphasise the real effectiveness of the LPV approach as well as its interest in the context of adaptation to varying processor or network load where a bank of switching controllers would need too much resources. In our case, using a single controller synthesis, the stability and performance property of the closed-loop system are guaranteed whatever the speed of variations of the sampling period are. In addition we also observed an interesting robustness of this controller w.r.t. sampling inaccuracies, e.g. which could be induced by preemptions in a multi-tasking operating systems. As shown in preliminary studies ([4, 13]), these properties are of prime interest in the design of more complex systems combining several such controllers under supervision of a feedback-scheduler : the control periods can be varied arbitrarily fast by an outer scheduling loop under a QoS objective with no risk of jeopardising the plants stability. However the specific robustness w.r.t. timing uncertainties deserve to be further investigated.

References

[1] A. Cervin and J. Eker, "Feedback scheduling of control tasks," in *Proceedings of the 39th IEEE Conference on Decision and Control*, Sydney, Australia, Dec. 2000.

[2] A. Cervin, J. Eker, B. Bernhardsson, and K.-E. Årzén, "Feedback-feedforward scheduling of control tasks," *Real-Time Systems*, vol. 23, no. 1–2, pp. 25–53, July 2002.

[3] J. Eker, P. Hagander, and K.-E. Årzén, "A feedback scheduler for real-time controller tasks," *Control Engineering Practice*, vol. 8, no. 12, pp. 1369–1378, Dec. 2000.

[4] D. Simon, D. Robert, and O. Sename, "Robust control/scheduling co-design: application to robot control," in *RTAS'05 IEEE Real-Time and Embedded Technology and Applications Symposium*, San Francisco, march 2005.

[5] D. Robert, O. Sename, and D. Simon, "Sampling period dependent rst controller used in control/scheduling co-design," in *Proceedings of the 16 th IFAC World Congress*, Czech Republic, July 2005.

[6] ——, "Synthesis of a sampling period dependent controller using LPV approach," in *5th IFAC Symposium on Robust Control Design ROCOND'06*, Toulouse, France, july 2006.

[7] P. Apkarian, P. Gahinet, and G. Becker, "Self-scheduled H_∞ control of linear parameter-varying systems: A design example," *Automatica*, vol. 31, no. 9, pp. 1251–1262, 1995.

[8] K. Tan, K.-M. Grigoriadis, and F. Wu, "Output-feedback control of LPV sampled-data systems," *Int. Journal of Control*, vol. 75, no. 4, pp. 252–264, 2002.

[9] K. J. Åström and B. Wittenmark, *Computer-Controlled Systems*, 3rd ed., ser. Information and systems sciences series. New Jersey: Prentice Hall, 1997.

[10] S. Boyd and L. Vandenberghe, *Convex Optimization*. Cambridge University Press, 2004.

[11] S. Skogestad and I. Postlethwaite, *Multivariable Feedback Control: analysis and design*. John Wiley and Sons, 1996.

[12] P. Gahinet and P. Apkarian, "A linear matrix inequality approach to h_∞ control," *International Journal of Robust and Nonlinear Control*, vol. 4, pp. 421–448, 1994.

[13] D. Robert, "Contribution to control and scheduling interaction," Ph.D. dissertation, INPG - Laboratoire d'Automatique de Grenoble (in french), january 11, 2007.

[14] J.-M. Biannic, "Commande robuste des systèmes à paramètres variables," Ph.D. dissertation, ENSAE, Toulouse, France, 1996.

[15] A. Zin, "On robust control of vehicle suspensions with a view to global chassis control," Ph.D. dissertation, INPG - Laboratoire d'Automatique de Grenoble, november 3, 2005.

[16] P. Gahinet, "Explicit controller formulas for LMI-based H_∞ synthesis," *Automatica*, vol. 32, no. 7, pp. 1007–14, 1996.

[17] M. Oliveira, J. Geromel, and J. Bernussou, "Extended h2 and hinf norm characterizations and controller parametrizations for discrete-time systems," *International Journal of Control*, vol. 75, no. 9, pp. 666–679, 2002.

Centre de recherche INRIA Grenoble – Rhône-Alpes
655, avenue de l'Europe - 38334 Montbonnot Saint-Ismier (France)

Centre de recherche INRIA Futurs : Parc Orsay Université - ZAC des Vignes
4, rue Jacques Monod - 91893 ORSAY Cedex
Centre de recherche INRIA Nancy – Grand Est : LORIA, Technopôle de Nancy-Brabois - Campus scientifique
615, rue du Jardin Botanique - BP 101 - 54602 Villers-lès-Nancy Cedex
Centre de recherche INRIA Rennes – Bretagne Atlantique : IRISA, Campus universitaire de Beaulieu - 35042 Rennes Cedex
Centre de recherche INRIA Paris – Rocquencourt : Domaine de Voluceau - Rocquencourt - BP 105 - 78153 Le Chesnay Cedex
Centre de recherche INRIA Sophia Antipolis – Méditerranée : 2004, route des Lucioles - BP 93 - 06902 Sophia Antipolis Cedex

Éditeur
INRIA - Domaine de Voluceau - Rocquencourt, BP 105 - 78153 Le Chesnay Cedex (France)
http://www.inria.fr
ISSN 0249-6399